Adaptive feedforward compensation algorithms for active vibration control with mechanical coupling

Ioan Doré Landau, Marouane Alma, Tudor-Bogdan Airimitoaie

Adaptive feedforward compensation algorithms for active vibration control with mechanical coupling ⋆

Ioan Doré Landau [a], Marouane Alma [a], Tudor-Bogdan Airimitoaie [a]

[a] *Control System Department of GIPSA-Lab, BP 46 St Martin d'Héres, 38402 FRANCE*

[b] *Facultatea de Automatica si Calculatoare, Universitatea "Politehnica" Bucuresti, Splaiul Independentei nr. 313, sector 6, 060042 Bucuresti*

Abstract

Adaptive feedforward broadband vibration (or noise) compensation is currently used when a correlated measurement with the disturbance (an image of the disturbance) is available. However in most of the systems there is a "positive" mechanical feedback coupling between the compensator system and the measurement of the image of the disturbance. This may lead to the instability of the system. The paper proposes new algorithms taking into account this coupling effect and provides the corresponding analysis. The algorithms have been applied to an active vibration control (AVC) system and real time results are presented. A theoretical and experimental comparison with some existing algorithms is also provided.

Key words: active vibration control, adaptive feedforward compensation, adaptive control, identification in closed loop, parameter estimation.

1 Introduction

Adaptive feedforward broadband vibration (or noise) compensation is currently used in ANC (Active Noise Control) and AVC (Active Vibration Control) when a correlated measurement with the disturbance (an image of the disturbance) is available ([4,5,10,19]). From the user point of view and taking into account the type of operation of adaptive disturbance compensation systems, one has to consider two modes of operation of the adaptive schemes:

- *Adaptive* operation. The adaptation is performed continuously with a non vanishing adaptation gain.
- *Self-tuning* operation. The adaptation procedure starts either on demand or when the performance is unsatisfactory. A vanishing adaptation gain is used.

At the end of the nineties it was pointed out that in many systems there is a "positive" feedback coupling between the compensator system and the measurement of the image of the disturbance. The positive feedback may destabilize the system. The system is no more a pure feedforward compensator. Different solutions have been proposed to overcome this problem ([8,19,7,9,10]).

One of the solutions to overcome this problem ([10]) is to try to compensate the positive feedback ([10,6]). However since the compensation can not be perfect, the potential instability of the system still exists ([18,3]).
Another approach discussed in the literature is the analysis in this new context of existing algorithms for adaptive feedforward compensation developed for the case without feedback. An attempt is made in [18] where the asymptotic convergence in a stochastic environment of the so called "Filtered-U LMS" (FULMS) algorithm is discussed. Further results on the same direction can be found in [6]. The authors use the Ljung's ODE method ([16]) for the case of a scalar vanishing adaptation gain. Unfortunately this is not enough because nothing is said about the stability of the system with respect to initial conditions and when a non vanishing adaptation gain is used (to keep adaptation capabilities). The authors assume that the positive feedback does not destabilize the system.

⋆ This paper was not presented at any IFAC meeting. Corresponding author I. D. Landau. Tel. +033-4-7682-6391. Fax +033-4-7682-6382.

Email addresses:
ioan-dore.landau@gipsa-lab.grenoble-inp.fr (Ioan Doré Landau),
marouane.alma@gipsa-lab.grenoble-inp.fr (Marouane Alma),
tudor-bogdan.airimitoaie@gipsa-lab.grenoble-inp.fr (Tudor-Bogdan Airimitoaie).

A stability approach for developing appropriate adaptive algorithms in the context of internal positive feedback is discussed in [8]. Unfortunately the results are obtained in the context of very particular assumptions upon the system, namely that the transfer function of the physical compensator system (called "secondary path" - see section 2) is strictly positive real, that the feedback path and the primary path (the transfer between the disturbance and the residual error) can be described by FIR (finite impulse response) models. Only the case of constant scalar adaption gain is considered. Convergence analysis in the stochastic case with a vanishing adaption gain is not provided.

An interesting approach is adopted in [19] using a Youla-Kucera parametrization (Q - parametrization) of the feedforward compensator. A fixed stabilizing feedforward filter is first designed and a recursive self-tuning procedure for estimating the Q filter is implemented using input-output data acquired without the compensator. Details are not given concerning a possible adaptive operation in the presence of the feedforward compensator. A stability analysis of the self-tuning algorithm is not provided.

The problem of the internal positive feedback can be properly addressed in the context of H_∞ or H_2 model based design. This approach has been considered in [3,17,1]. However the resulting compensator does not have adaptation capabilities and its performance is not necessarily very good. Provided that the high dimension of the resulting compensator can be reduced, it may constitute an "initial" value for the parameters of an adaptive or self-tuning feedforward compensator. In [3] it is shown experimentally that the results obtained with the H_∞ approach are better than those obtained using the very popular FULMS adaptation algorithm (for a disturbance with known spectral characteristics). A similar comparison done experimentally in this paper confirms this fact. However this is no more true when comparing the H_∞ design with the adaptive algorithms introduced in the present paper (see section 7).
It is important to remark that all these contributions (except [1]) have been done in the context of active noise control. While the algorithms for active noise control can be used in active vibration control, one has to take into account the specificity of these latter systems which feature many low damped vibration modes (resonance) and low damped complex zeros (anti-resonance).

The main contributions of the present paper are:

- development of new real time recursive adaptation algorithms for active vibration control systems with mechanical coupling.
- stability analysis (in a deterministic context) and convergence analysis (in a stochastic context) of the algorithms.
- application of the algorithms to an active vibration control system (most of the available control literature deal only with active noise control).
- comparison of the new algorithms with existing algorithms (both theoretically and experimentally).

While the algorithms have been developed in the context of AVC, they are certainly applicable to ANC systems with acoustic coupling.

The paper is organized as follows. The AVC system on which the algorithms will be tested, is presented in section 2. The system representation and feedforward compensator structure are given in section 3. The algorithm for adaptive feedforward compensation will be developed in section 4 and analysed in section 5. Section 6 will present a comparison with other algorithms. Section 7 will present experimental results obtained on the active vibration control system with the algorithms introduced in this paper as well as with two other adaptive algorithms given in the literature.

2 An active vibration control system using an inertial actuator

Figures 1 and 2 represent an AVC system using a correlated measurement with the disturbance and an inertial actuator for reducing the residual acceleration. The structure is representative for a number of situations encountered in practice.

The system consists of three mobile metallic plates (M1, M2, M3) connected by springs. The first and the third plates are also connected by springs to the rigid part of the system formed by two other metallic plates connected themselves rigidly. The upper and lower mobile plates (M1 and M3) are equipped with inertial actuators. The one on the top serves as disturbance generator (inertial actuator 1 in figure 2), the one at the bottom serves for disturbance compensation (inertial actuator 2 in figure 2). The system is equipped with a measure of the residual acceleration (on plate M3) and a measure of the image of the disturbance made by an accelerometer posed on plate M1. The path between the disturbance (in this case, generated by the inertial actuator on top of the structure), and the residual acceleration is called the *global primary path*. The path between the measure of the image of the disturbance and the residual acceleration (in open loop) is called the *primary path* and the path between the inertial actuator for compensation and the residual acceleration is called the *secondary path*. When the compensator system is active, the actuator acts upon the residual acceleration, but also upon the measurement of the image of the disturbance (a positive feedback). The measured quantity $\widehat{u}(t)$ will be the sum of the correlated disturbance measurement $d(t)$ obtained in the absence of the feedforward compensation (see figure 3(a)) and of the effect of the actuator used for compensation.

The disturbance is the position of the mobile part of the inertial actuator (see figures 1 and 2) located on top of the structure. The input to the compensator system is the position of the mobile part of the inertial actuator located on the bottom of the structure.

The input to the inertial actuators being a position, the global primary path, the secondary path and the positive feedback

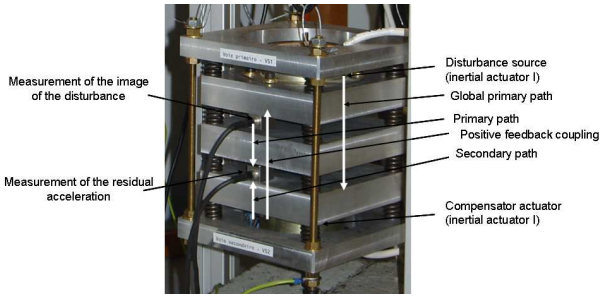

Fig. 1. An AVC system using a feedforward compensation - photo

path have a double differentiator behavior.

The corresponding block diagrams in open loop operation and with the compensator system are shown in Figures 3(a) and 3(b), respectively. In figure 3(b), $\hat{u}(t)$ denotes the effective output provided by the measurement device and which will serve as input to the adaptive feedforward filter $\hat{N}$. The output of this filter denoted by $\hat{y}(t)$ is applied to the actuator through an amplifier. The transfer function G (the secondary path) characterizes the dynamics from the output of the filter $\hat{N}$ to the residual acceleration measurement (amplifier + actuator + dynamics of the mechanical system). The transfer function D between $d(t)$ and the measurement of the residual acceleration (in open loop operation) characterizes the primary path.

The coupling between the output of the filter and the measurement $\hat{u}(t)$ through the compensator actuator is denoted by M. As indicated in figure 3(b) this coupling is a "positive" feedback. This unwanted coupling raises problems in practice (source of instabilities) and makes the analysis of adaptive (estimation) algorithms more difficult.

At this stage it is important to make the following remarks, when the feedforward filter is absent (open loop operation):

- very reliable models for the secondary path and the "positive" feedback path can be identified by applying appropriate excitation on the actuator.
- an estimation of the primary path transfer function can be obtained using the measured $d(t)$ as input and $\chi(t)$ as

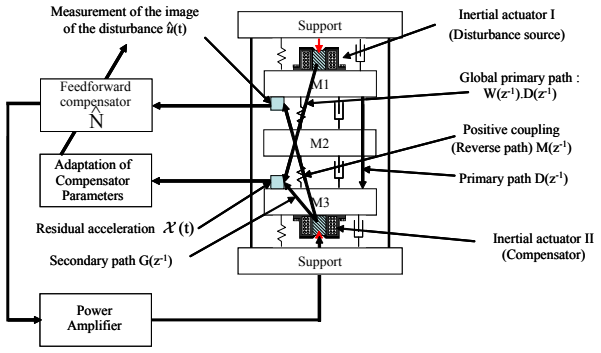

Fig. 2. An AVC system using a feedforward compensation - scheme

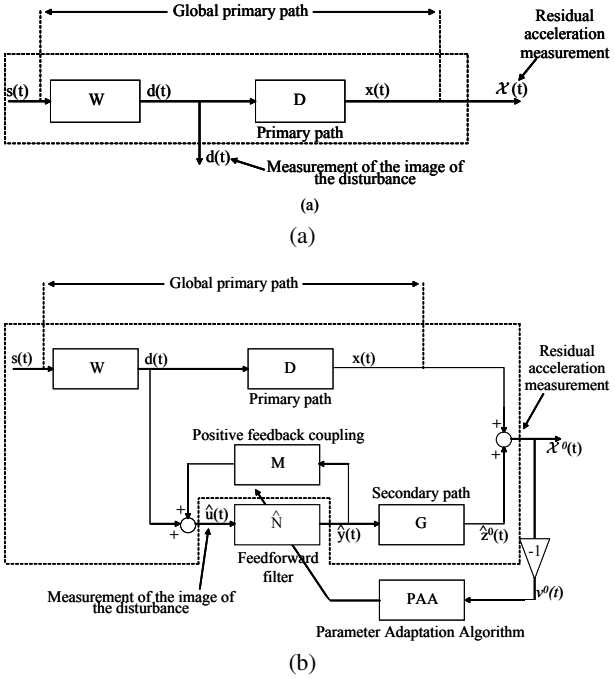

Fig. 3. Feedforward AVC: in open loop (a) and with adaptive feedforward compensator (b)

output (the compensator actuator being at rest).

The objective is to develop stable recursive algorithms for online estimation and adaptation of the parameters of the feedforward filter compensator (which will be denoted $\hat{N}$) such that the measured residual error (acceleration or force in AVC, noise in ANC) be minimized in the sense of a certain criterion. This has to be done for broadband disturbances $d(t)$ (or $s(t)$) with unknown and variable spectral characteristics and an unknown primary path model. [1] .

3 Basic Equations and Notations

The description of the various blocks will be made with respect to Figure 3.

The primary path is characterized by the asymptotically stable transfer operator [2] :

$$D(q^{-1}) = \frac{B_D(q^{-1})}{A_D(q^{-1})} \tag{1}$$

where

$$B_D(q^{-1}) = b_1^D q^{-1} + \ldots + b_{n_{B_D}}^D q^{-n_{B_D}} \tag{2}$$

[1] Variations of the unknown model W, the transfer function between the disturbance $s(t)$ and $d(t)$ are equivalent to variations of the spectral characteristics of $s(t)$.

[2] The complex variable z^{-1} will be used for characterizing the system's behavior in the frequency domain and the delay operator q^{-1} will be used for describing the system's behavior in the time domain.

$$A_D(q^{-1}) = 1 + a_1^D q^{-1} + ... + a_{n_{A_D}}^D q^{-n_{A_D}} \quad (3)$$

The unmeasurable value of the output of the primary path (when the compensation is active) is denoted $x(t)$.
The secondary path is characterized by the asymptotically stable transfer operator:

$$G(q^{-1}) = \frac{B_G(q^{-1})}{A_G(q^{-1})} \quad (4)$$

where:

$$B_G(q^{-1}) = b_1^G q^{-1} + ... + b_{n_{B_G}}^G q^{-n_{B_G}} = q^{-1} B_G^*(q^{-1}) \quad (5)$$

$$A_G(q^{-1}) = 1 + a_1^G q^{-1} + ... + a_{n_{A_G}}^G q^{-n_{A_G}} \quad (6)$$

The positive feedback coupling is characterized by the asymptotically stable transfer operator:

$$M(q^{-1}) = \frac{B_M(q^{-1})}{A_M(q^{-1})} \quad (7)$$

where:

$$B_M(q^{-1}) = b_1^M q^{-1} + ... + b_{n_{B_M}}^M q^{-n_{B_M}} = q^{-1} B_M^*(q^{-1}) \quad (8)$$

$$A_M(q^{-1}) = 1 + a_1^M q^{-1} + ... + a_{n_{A_M}}^M q^{-n_{A_M}} \quad (9)$$

Both B_G and B_M have a one step discretization delay. The identified models of the secondary path and of the positive feedback coupling will be denoted $\hat{G}$ and $\hat{M}$, respectively.
The optimal feedforward filter (unknown) is defined by :

$$N(q^{-1}) = \frac{R(q^{-1})}{S(q^{-1})} \quad (10)$$

where:

$$R(q^{-1}) = r_0 + r_1 q^{-1} + ... + r_{n_R} q^{-n_R} \quad (11)$$

$$S(q^{-1}) = 1 + S_1 q^{-1} + ... + S_{n_S} q^{-n_S} = 1 + q^{-1} S^*(q^{-1}) \quad (12)$$

The estimated filter is denoted by $\hat{N}(q^{-1})$ or $\hat{N}(\hat{\theta}, q^{-1})$ when it is a linear filter with constant coefficients or $\hat{N}(t, q^{-1})$ during estimation (adaptation) of its parameters.

The input of the feedforward filter is denoted by $\hat{u}(t)$ and it corresponds to the measurement provided by the primary transducer (force or acceleration transducer in AVC or a microphone in ANC). In the absence of the compensation loop (open loop operation) $\hat{u}(t) = d(t)$. The "a posteriori" output of the feedforward filter (which is the control signal applied to the secondary path) is denoted by $\hat{y}(t+1) = \hat{y}(t+1|\hat{\theta}(t+1))$. The "a priori" output of the estimated feedforward filter is given by:

$$\begin{aligned} \hat{y}^0(t+1) &= \hat{y}(t+1|\hat{\theta}(t)) \\ &= -\hat{S}^*(t, q^{-1})\hat{y}(t) + \hat{R}(t, q^{-1})\hat{u}(t+1) \\ &= \hat{\theta}^T(t)\phi(t) = \left[\hat{\theta}_S^T(t), \hat{\theta}_R^T(t)\right] \begin{bmatrix} \phi_{\hat{y}}(t) \\ \phi_{\hat{u}}(t) \end{bmatrix} \end{aligned} \quad (13)$$

where

$$\hat{\theta}^T(t) = [\hat{s}_1(t)...\hat{s}_{n_S}(t), \hat{r}_0(t)...\hat{r}_{n_R}(t)] = [\hat{\theta}_S^T(t), \hat{\theta}_R^T(t)] \quad (14)$$

$$\begin{aligned} \phi^T(t) &= [-\hat{y}(t)... - \hat{y}(t - n_S + 1, \hat{u}(t+1), \hat{u}(t)...\hat{u}(t - n_R + 1)] \\ &= [\phi_{\hat{y}}^T(t), \phi_{\hat{u}}^T(t)] \end{aligned} \quad (15)$$

and $\hat{y}(t)$, $\hat{y}(t-1)$ ... are the "a posteriori" outputs of the feedforward filter generated by:

$$\hat{y}(t+1) = \hat{y}(t+1|\hat{\theta}(t+1)) = \hat{\theta}^T(t+1)\phi(t) \quad (16)$$

while $\hat{u}(t+1)$, $\hat{u}(t)$... are the measurements provided by the primary transducer [3] . The unmeasurable "a priori" output of the secondary path will be denoted $\hat{z}^0(t+1)$.

$$\hat{z}^0(t+1) = \hat{z}(t+1|\hat{\theta}(t)) = \frac{B_G^*(q^{-1})}{A_G(q^{-1})}\hat{y}(t) \quad (17)$$

The "a posteriori" unmeasurable value of the output of the secondary path is denoted by:

$$\hat{z}(t+1) = \hat{z}(t+1|\hat{\theta}(t+1)) \quad (18)$$

The measured primary signal (called also reference) satisfies the following equation:

$$\hat{u}(t+1) = d(t+1) + \frac{B_M^*(q^{-1})}{A_M(q^{-1})}\hat{y}(t) \quad (19)$$

The measured residual error satisfies the following equation:

$$\chi^0(t+1) = \chi(t+1|\hat{\theta}(t)) = \hat{z}^0(t+1) + x(t+1) \quad (20)$$

The "a priori" adaptation error is defined as:

$$\nu^0(t+1) = -\chi^0(t+1) = -x(t+1) - \hat{z}^0(t+1) \quad (21)$$

The "a posteriori" adaptation (residual) error (which is computed) will be given by:

$$\nu(t+1) = \nu(t+1|\hat{\theta}(t+1)) = -x(t+1) - \hat{z}(t+1) \quad (22)$$

When using an estimated filter $\hat{N}$ with constant parameters: $\hat{y}^0(t) = \hat{y}(t)$, $\hat{z}^0(t) = \hat{z}(t)$ and $\nu^0(t) = \nu(t)$.

[3] $\hat{u}(t+1)$ is available before adaptation of parameters starts at $t+1$

4 Development of the Algorithms

The algorithms for adaptive feedforward compensation will be developed under the following hypotheses:

(1) H1 - The signal $d(t)$ is bounded
i.e.
$$|d(t)| \leq \alpha \quad \forall t \quad (0 \leq \alpha \leq \infty) \tag{23}$$
(which is equivalently to say that $s(t)$ is bounded and $W(q^{-1})$ in figure 3 is asymptotically stable).

(2) H2 - Perfect matching condition. There exists a filter $N(q^{-1})$ of finite dimension such that [4]:
$$D = -\frac{N}{(1-NM)}G \tag{24}$$
and the characteristic polynomial of the "internal" feedback loop:
$$P(z^{-1}) = A_M(z^{-1})S(z^{-1}) - B_M(z^{-1})R(z^{-1}) \tag{25}$$
is a Hurwitz polynomial.

(3) H3 - The effect of the measurement noise upon the measured residual error is neglected (deterministic context).

(4) H4 - The primary path model $D(z^{-1})$ is unknown and constant

Once the algorithms will be developed under these hypotheses, hypotheses 2 and 3 will be removed and the algorithms will be analyzed in this modified context.
A first step in the development of the algorithms is to establish a relation between the errors on the estimation of the parameters of the feedforward filter and the measured residual acceleration. This is summarized in the following lemma.

Lemma 4.1: *Under hypotheses H1 through H4, for the system described by equations (1) through (22) using a feedforward compensator $\hat{N}$ with constant parameters, one has:*

$$\nu(t+1) = \frac{A_M(q^{-1})G(q^{-1})}{P(q^{-1})}[\theta - \hat{\theta}]^T \phi(t) \tag{26}$$

where

$$\theta^T = [s_1, ...s_{n_S}, r_0, r_1, ...r_{n_R}] = [\theta_S^T, \theta_R^T] \tag{27}$$

is the vector of parameters of the optimal filter N assuring perfect matching

$$\hat{\theta}^T = [\hat{s}_1 ...\hat{s}_{n_S}, \hat{r}_0 ...\hat{r}_{n_R}] = [\hat{\theta}_S^T, \hat{\theta}_R^T] \tag{28}$$

is the vector of constant estimated parameters of $\hat{N}$ and $\phi(t)$ and $\hat{u}(t+1)$ are given by 15 and 19.

[4] In many cases, the argument q^{-1} or z^{-1} will be dropped out

The proof of this lemma is given in Appendix 1.
Filtering the vector $\phi(t)$ through an asymptotically stable filter $L(q^{-1}) = \frac{B_L}{A_L}$, equation (26) for $\hat{\theta} =$ constant becomes:

$$\nu(t+1) = \frac{A_M(q^{-1})G(q^{-1})}{P(q^{-1})L(q^{-1})}[\theta - \hat{\theta}]^T \phi_f(t) \tag{29}$$

with:
$$\phi_f(t) = L(q^{-1})\phi(t) \tag{30}$$
Equation (29) will be used to develop the adaptation algorithms neglecting for the moment the non-commutativity of the operators when $\hat{\theta}$ is time varying (however an exact algorithm can be derived in such cases - see [**?**]).

Replacing the fixed estimated parameters by the current estimated parameters, equation (29) becomes the equation or the a-posteriori residual error $\nu(t+1)$ (which is computed):

$$\nu(t+1) = \frac{A_M(q^{-1})G(q^{-1})}{P(q^{-1})L(q^{-1})}[\theta - \hat{\theta}(t+1)]^T \phi_f(t) \tag{31}$$

Equation (31) has the standard form for an a-posteriori adaptation error ([**?**]), which immediately suggests to use the following parameter adaptation algorithm:

$$\hat{\theta}(t+1) = \hat{\theta}(t) + F(t)\psi(t)\nu(t+1) \; ; \tag{32}$$
$$\nu(t+1) = \frac{\nu^0(t+1)}{1 + \psi^T(t)F(t)\psi(t)} \; ; \tag{33}$$
$$F(t+1) = \frac{1}{\lambda_1(t)}\left[F(t) - \frac{F(t)\psi(t)\psi^T(t)F(t)}{\frac{\lambda_1(t)}{\lambda_2(t)} + \psi^T(t)F(t)\psi(t)}\right] \tag{34}$$
$$1 \geq \lambda_1(t) > 0; 0 \leq \lambda_2(t) < 2; F(0) > 0 \tag{35}$$
$$\psi(t) = \phi_f(t) \tag{36}$$

where $\lambda_1(t)$ and $\lambda_2(t)$ allow to obtain various profiles for the matrix adaptation gain $F(t)$ (see section 7 and [**?**]). By taking $\lambda_2(t) \equiv 0$ and $\lambda_1(t) \equiv 1$, one gets a constant adaptation gain matrix (and choosing $F = \gamma I$, $\gamma > 0$ one gets a scalar adaptation gain).

Three choices for the filter L will be considered, leading to three different algorithms:
Algorithm *I*: $L = G$
Algorithm *II*: $L = \hat{G}$
Algorithm *III*:
$$L = \frac{\hat{A}_M}{\hat{P}}\hat{G} \tag{37}$$
where:
$$\hat{P} = \hat{A}_M\hat{S} - \hat{B}_M\hat{R} \tag{38}$$
is an estimation of the characteristic polynomial of the internal feedback loop computed on the basis of available estimates of the parameters of the filter $\hat{N}$.
For the Algorithm *III* several otions for updating $\hat{P}$ can be considered:

- Run Algorithm *II* for a certain time to get estimates of $\hat{R}$ and $\hat{S}$
- Run a simulation (using the identified models)
- Update $\hat{P}$ at each sampling instant or from time to time using Algorithm *III* (after a short initialization horizon using Algorithm *II*)

The following procedure is applied at each sampling time for *adaptive* or *self-tuning* operation:

(1) Get the measured image of the disturbance $\hat{u}(t+1)$, the measured residual error $\chi^0(t+1)$ and compute $\nu^0(t+1) = -\chi^0(t+1)$
(2) Compute $\phi(t)$ and $\phi_f(t)$ using (15) and (30)
(3) Estimate the parameter vector $\hat{\theta}(t+1)$ using the parametric adaptation algorithm (32) through (36).
(4) Compute (using (16)) and apply the control.

5 Analysis of the Algorithms

5.1 The Deterministic Case - Perfect Matching

For algorithms I, II and III the equation for the a-posteriori adaptation error has the form:

$$\nu(t+1) = H(q^{-1})[\theta - \hat{\theta}(t+1)]^T \psi(t) \tag{39}$$

where:

$$H(q^{-1}) = \frac{A_M(q^{-1})G(q^{-1})}{P(q^{-1})L(q^{-1})}, \psi = \phi_f \tag{40}$$

Neglecting the non-commutativity of time varying operators, one has the following result:

Lemma 5.1: *Assuming that eq. (39) represents the evolution of the a posteriori adaptation error and that the parameter adaptation algorithm (32) through (36) is used, one has*:

$$\lim_{t\to\infty} \nu(t+1) = 0 \tag{41}$$

$$\lim_{t\to\infty} \frac{[\nu^0(t+1)^2]}{1+\psi(t)^T F(t)\psi(t)} = 0 \tag{42}$$

$$||\psi(t)|| \text{ is bounded} \tag{43}$$

$$\lim_{t\to\infty} \nu^0(t+1) = 0 \tag{44}$$

for any initial conditions $\hat{\theta}(0), \nu^0(0), F(0)$, *provided that:*

$$H'(z^{-1}) = H(z^{-1}) - \frac{\lambda_2}{2}, \max_t [\lambda_2(t)] \le \lambda_2 < 2 \tag{45}$$

is a strictly positive real transfer function.

Proof: Using Theorem 3.2 from [**?**], under the condition (45), (41) and (42) hold.

However in order to show that $\nu^0(t+1)$ goes to zero one has to show first that the components of the observation vector are bounded. The result (42) suggests to use the Goodwin's "bounded growth" lemma ([13] and Lemma 11.1 in [**?**]).

Provided that one has:

$$|\psi^T(t)F(t)\psi(t)|^{\frac{1}{2}} \le C_1 + C_2 \cdot \max_{0\le k\le t+1} |\nu^0(k)| \tag{46}$$

$$0 < C_1 < \infty \qquad 0 < C_2 < \infty \qquad F(t) > 0$$

$||\psi(t)||$ will be bounded. So it will be shown that (46) holds for algorithm I (for algorithms II and III the proof is similar). From (22) one has:

$$-\hat{z}(t) = \nu(t) + x(t) \tag{47}$$

Since $x(t)$ is bounded (output of an asymptotically stable system with bounded input), one has:

$$|-\hat{y}_f(t)| = |-G\hat{y}(t)| = |-\hat{z}(t)| \le C_3 + C_4 \cdot \max_{0\le k\le t+1} |\nu(k)|$$

$$\le C_3' + C_4' \cdot \max_{0\le k\le t+1} |\nu^0(k)| \tag{48}$$

$$0 < C_3, C_4, C_3', C_4' < \infty \tag{49}$$

since $|\nu(t)| \le |\nu^0(t)|$ for all t. Filtering both sides of equation (19) by $G(q^{-1})$ one gets in the adaptive case:

$$\hat{u}_f(t) = \frac{B_G}{A_G} d(t) + \frac{B_M}{A_M} \hat{y}_f(t) \tag{50}$$

Since A_G and A_M are Hurwitz polynomials and $d(t)$ is bounded, it results that:

$$|\hat{u}_f(t)| \le C_5 + C_6 \cdot \max_{0\le k\le t+1} |\nu^0(k)|; \qquad 0 < C_5, C_6 < \infty \tag{51}$$

Therefore (46) holds, which implies that $\psi(t)$ is bounded and one can conclude that (44) also holds. End of the proof.

It is interesting to remark that for Algorithm *III* taking into account equation (37), the stability condition is that:

$$\frac{A_M}{\hat{A}_M} \cdot \frac{\hat{P}}{P} \cdot \frac{G}{\hat{G}} - \frac{\lambda_2}{2} \tag{52}$$

should be a strictly positive real transfer function. However this condition can be re-written for $\lambda_2 = 1$ as ([16,15]):

$$\left| \left(\frac{A_M}{\hat{A}_M} \cdot \frac{\hat{P}}{P} \cdot \frac{G}{\hat{G}} \right)^{-1} - 1 \right| < 1 \tag{53}$$

for all ω. This roughly means that it always holds provided that the estimates of A_M, P, and G are close to the true values (i.e. $H(e^{j\omega})$ in this case is close to a unit transfer function).

5.2 The Stochastic Case - Perfect Matching

There are two sources of measurement noise, one acting on the primary transducer which gives the correlated measurement with the disturbance and the second acting on the measurement of the residual error (force, acceleration). For the primary transducer the effect of the measurement noise is negligible since the signal to noise ratio is very high. The situation is different for the residual error where the effect of the noise can not be neglected.

In the presence of the measurement noise (w), the equation of the a-posteriori residual error becomes:

$$\nu(t+1) = H(q^{-1})[\theta - \hat{\theta}(t+1)]^T \psi(t) + w(t+1) \quad (54)$$

The O.D.E. method [16,15] can be used to analyse the asymptotic behavior of the algorithm in the presence of noise. Taking into account the form of equation (54), one can directly use theorem 4.1 of [**?**] or theorem B1 of [12].

The following assumptions will be made:

(1) $\lambda_1(t) = 1$ and $\lambda_2(t) = \lambda_2 > 0$
(2) $\hat{\theta}(t)$ generated by the algorithm belongs infinitely often to the domain D_S:

$$D_S \triangleq \{\hat{\theta} : \hat{P}(z^{-1}) = 0 \Rightarrow |z| < 1\}$$

for which stationary processes:

$$\psi(t,\hat{\theta}) \triangleq \psi(t)|_{\hat{\theta}(t)=\hat{\theta}=const}$$
$$\chi(t,\hat{\theta}) = \chi(t)|_{\hat{\theta}(t)=\hat{\theta}=const}$$

can be defined.
(3) $w(t)$ is a zero mean stochastic process with finite moments and independent of the sequence $d(t)$.

From (54) for $\hat{\theta}(t) = \hat{\theta}$, one gets:

$$\nu(t+1,\hat{\theta}) = H(q^{-1})[\theta - \hat{\theta}]^T \psi(t,\hat{\theta}) + w(t+1,\hat{\theta}) \quad (55)$$

Since $\psi(t,\hat{\theta})$ depends upon $d(t)$ one concludes that $\psi(t,\hat{\theta})$ and $w(t+1,\hat{\theta})$ are independent. Therefore using Theorem 4.1 from [**?**] it results that if:

$$H'(z^{-1}) = \frac{A_M(z^{-1})G(z^{-1})}{P(z^{-1})L(z^{-1})} - \frac{\lambda_2}{2} \quad (56)$$

is a strictly positive real transfer function, one has: $Prob\{\lim_{t\to\infty} \hat{\theta}(t) \in D_C\} = 1$
where: $D_C = \{\hat{\theta} : \psi^T(t,\hat{\theta})(\theta - \hat{\theta}) = 0\}$.
If furthermore $\psi^T(t,\hat{\theta})(\theta - \hat{\theta}) = 0$ has a unique solution (richness condition), the condition that $H'(z^{-1})$ be strictly positive real implies that: $Prob\{\lim_{t\to\infty} \hat{\theta}(t) = \theta\} = 1$.

5.3 The Case of Non-Perfect Matching

If $\hat{N}(t,q^{-1})$ does not have the appropriate dimension there is no chance to satisfy the perfect matching condition.
Two questions are of interest in this case:

(1) The boundedness of the residual error
(2) The bias distribution in the frequency domain

5.3.1 Boundedness of the residual error

For analyzing the boundedness of the residual error, results from [12,13], can be used. The following assumptions are made:

(1) There exists a reduced order filter $\hat{N}$ characterized by the unknown polynomials $\hat{S}$ (of order n_S) and $\hat{R}$ (of order n_R), for which the closed loop formed by $\hat{N}$ and M is asymptotically stable. i.e. $A_M\hat{S} - B_M\hat{R}$ is a Hurwitz polynomial.
(2) The output of the optimal filter satisfying the matching condition can be expressed as:

$$\hat{y}(t+1) = -[\hat{S}^*(q^{-1})\hat{y}(t) - \hat{R}(q^{-1})\hat{u}(t+1) + \eta(t+1)] \quad (57)$$

where $\eta(t+1)$ is a norm bounded signal

Using the results of [12] (theorem 4.1 pp 1505-1506) and assuming that $d(t)$ is norm bounded, it can be shown that all the signals are norm bounded under the passivity condition (45), where P is computed now with the reduced order estimated filter.

5.3.2 Bias distribution

Using the Parseval's relation, the asymptotic bias distribution of the estimated parameters in the frequency domain can be obtained starting from the expression of $\nu(t)$, by taking into account that the algorithm minimizes (almost) a criterion of the form $\lim_{N\to\infty} \frac{1}{N}\sum_{t=1}^{N} \nu^2(t)$.
The bias distribution (for algorithm *III*) will be given by:

$$\hat{\theta}^* = \arg\min_{\hat{\theta}} \int_{-\pi}^{\pi} [|D(j\omega) - \frac{\hat{N}(j\omega)G(j\omega)}{1 - \hat{N}(j\omega)M(j\omega)}|^2 \phi_d(\omega) + \phi_w(\omega)] d\omega \quad (58)$$

where ϕ_d and ϕ_w are the spectral densities of the disturbance $d(t)$ and of the measurement noise. Taking into account equation (24), one obtains:

$$\hat{\theta}^* = \arg\min_{\hat{\theta}} \int_{-\pi}^{\pi} [|S_{NM}|^2 |N - \hat{N}|^2 |S_{\hat{N}M}|^2 |G|^2 \phi_d(\omega) + \phi_w(\omega)] d\omega \quad (59)$$

where S_{NM} and $S_{\hat{N}M}$ are the output sensitivity functions of the internal closed loop for N and respectively $\hat{N}$: $S_{NM} = \frac{1}{1-NM}; S_{\hat{N}M} = \frac{1}{1-\hat{N}M}$.

From (58) and (59) one concludes that a good approximation of N will be obtained in the frequency region where ϕ_d is significant and where G has a high gain (usually G should have high gain in the frequency region where ϕ_d is significant in order to counteract the effect of $d(t)$). However the quality of the estimated $\hat{N}$ will be affected also by the output sensitivity functions of the internal closed loop $N-M$.

5.4 Relaxing the Positive Real Condition

It is possible to relax the strictly positive real (S.P.R.) conditions taking into account that:

(1) The disturbance (input to the system) is a broadband signal
(2) Most of the adaptation algorithms work with a low adaptation gain.

Under these two assumptions, the behavior of the algorithm can be well described by the "averaging theory" developed in Anderson and al. [2] and Ljung [16] (see also [**?**]).

When using the averaging approach, the basic assumption of a slow adaptation holds for small adaptation gains (constant and scalar in [2] i.e. $\lambda_2(t) \equiv 0, \lambda_1(t) = 1$; matrix and time decreasing asymptotically in [16,**?**] i.e $\lim_{t\to\infty} \lambda_1(t) = 1, \lambda_2(t) = \lambda_2 > 0$ or scalar and time decreasing.).
In the context of averaging, the basic condition for stability is that:

$$\lim_{N\to\infty} \frac{1}{N} \sum_{t=1}^{N} \psi(t)\, H'(q^{-1}) \psi^T(t) = \frac{1}{2} \int_{-\pi}^{\pi} \psi(e^{j\omega}) [H'(e^{j\omega}) + H'(e^{-j\omega})] \psi^T(e^{-j\omega}) d\omega > 0 \qquad (60)$$

be a positive definite matrix ($\psi(e^{j\omega})$ is the Fourier transform of $\psi(t)$).
One can view (60) as the weighted energy of the observation vector ψ. Of course the S.P.R sufficient condition upon $H'(z^{-1})$ (see Equation 45) allows to satisfy this condition. However in the averaging context it is only needed that (60) is true which allows that H' be non positive real in a limited frequency band. Expression (60) can be re-written as follows:

$$\int_{-\pi}^{\pi} \psi(e^{j\omega}) [H' + H'^*] \psi^T(e^{-j\omega}) d\omega = \sum_{i=1}^{r} \int_{\alpha_i}^{\alpha_i+\Delta_i} \psi(e^{j\omega}) [H' + H'^*] \psi^T(e^{-j\omega}) d\omega - \sum_{j=1}^{p} \int_{\beta_j}^{\beta_j+\Delta_j} \psi(e^{j\omega}) [\bar{H}' + \bar{H}'^*] \psi^T(e^{-j\omega}) d\omega > 0 \qquad (61)$$

where H' is strictly positive real in the frequency intervals $[\alpha_i, \alpha_i + \Delta_i]$ and $\bar{H}' = -H'$ is positive real in the frequencies intervals $[\beta_j, \beta_j + \Delta_j]$ (H'^* denotes the complex conjugate of H'). The conclusion is that H' does not need to be S.P.R. It is enough that the "positive" weighted energy exceeds the "negative" weighted energy. This explains why algorithms *I* and *II* will work in practice in most of the cases. It is however important to remark that if the disturbance is a single sinusoid (which violates the hypothesis of broadband disturbance) located in the frequency region where H' is not S.P.R, the algorithm may diverge (see [2,16]).

Without doubt, the best approach for relaxing the S.P.R. conditions, is to use algorithm *III* (given in eq.(37)) instead of algorithm *II*. This is motivated by equations (52) and (53). As it will be shown experimentally, this algorithm gives the best results.

6 Comparison with other algorithms

The algorithms developed in this paper with matrix and scalar adaptation gain for IIR feedforward compensators will be compared with the algorithm of Jacobson-Johnson ([8]) and the FULMS ([18]) algorithm. These two references consider the same type of compensator and take into account the internal positive feedback [5] .

Table 1 summarizes the structure of the algorithms, the stability and convergence conditions as well as the hypotheses upon the structure of the system. The notations adopted in this paper were used to describe the other algorithms. A table in Appendix 2 gives the equivalence of the notations between the present paper and the notations used in [8] and [18]. It was not possible to give in table 1 all the options for the adaptation gain. However basic characteristics for adaptive operation (non vanishing adaptation gain) and self-tuning operation (vanishing adaptation gain) have been provided [6] .

7 Experimental results

A detailed view of the mechanical structure used for the experiments has been given in figure 1 and the description of the system has been given in section 2.

7.1 System identification

The models of the plant may be obtained by parametric system identification with the same methodology used for an active suspension in [13,11].

The secondary path between the control signal $\hat{y}(t)$ and the output $\chi(t)$ has been identified in the absence of the feedforward compensator. The excitation signal was a PRBS generated with a shift register with $N = 10$ and a frequency divider

[5] Algorithms dedicated to FIR feedforward compensators have not been considered because they are particular cases of the algorithms for IIR compensators.

[6] Convergence analysis can be applied only for vanishing adaptation gains.

	Paper (Matrix gain)	Paper (Scalar gain)	Jacobson-Johnson(Scalar gain)	FULMS (Scalar gain)
$\hat{\theta}(t+1) =$	$\hat{\theta}(t)+F(t)\psi(t)\frac{v^0(t+1)}{1+\psi^T(t)F(t)\psi(t)}$	$\hat{\theta}(t)+\gamma(t)\psi(t)\frac{v^0(t+1)}{1+\gamma(t)\psi^T(t)\psi(t)}$	$\hat{\theta}(t)+\mu\gamma\psi(t)\frac{v^0(t+1)}{1+\gamma\psi^T(t)\psi(t)}$	$\hat{\theta}(t)+\gamma(t)\psi(t-1)v^0(t)$
Adapt. gain	$F(t+1)^{-1}=\lambda_1(t)F(t)+$ $+\lambda_2(t)\psi(t)\psi^T(t)$ $0\le\lambda_1(t)<1, 0\le\lambda_2(t)<2$ $F(0)>0$	$\gamma(t)>0$	$\gamma>0, \quad 0<\mu\le 1$	$\gamma(t)>0$
Adaptive	Decr. gain and const. trace	$\gamma(t)=\gamma=const$	$\gamma>0$	$\gamma(t)=\gamma=const$
Self tuning	$\lambda_2=const.$ $\lim_{t\to\infty}\lambda_1(t)=1$	$\sum_{t=1}^{\infty}\gamma(t)=\infty, \quad \lim_{t\to\infty}\gamma(t)=0$	Does not apply	$\sum_{t=1}^{\infty}\gamma(t)=\infty, \quad \lim_{t\to\infty}\gamma(t)=0$
$\phi^T(t) =$	$[-\hat{y}(t),\ldots,\hat{u}(t+1),\ldots]$	$[-\hat{y}(t),\ldots,\hat{u}(t+1),\ldots]$	$[-\hat{y}(t),\ldots,\hat{u}(t+1),\ldots]$	$[-\hat{y}(t),\ldots,\hat{u}(t+1),\ldots]$
$\psi(t) =$	$L\phi(t)$ $L_2=\hat{G}; \quad L_3=\frac{\hat{A}_M}{\hat{P}}\hat{G}$ $\hat{P}=\hat{A}_M\hat{S}-\hat{B}_M\hat{R}$	$L\phi(t)$ $L_2=\hat{G}; \quad L_3=\frac{\hat{A}_M}{\hat{P}}\hat{G}$ $\hat{P}=\hat{A}_M\hat{S}-\hat{B}_M\hat{R}$	$\phi(t)$	$L\phi(t)$ $L=\hat{G}$
$G=\frac{B_G}{A_G}$	$B_G=b_{1_G}z^{-1}+b_{2_G}z^{-2}+\ldots$ $A_G=1+a_{1_G}z^{-1}+a_{2_G}z^{-2}+\ldots$	$B_G=b_{1_G}z^{-1}+b_{2_G}z^{-2}+\ldots$ $A_G=1+a_{1_G}z^{-1}+\ldots$	$B_G=1, \quad A_G=1$ or $G=SPR$	$B_G=b_{1_G}z^{-1}+b_{2_G}z^{-2}+\ldots$ $A_G=1+a_{1_G}z^{-1}+\ldots$
$M=\frac{B_M}{A_M}$	$B_M=b_{1_M}z^{-1}+b_{2_M}z^{-2}+\ldots$ $A_M=1+a_{1_M}z^{-1}+a_{2_M}z^{-2}+\ldots$	$B_M=b_{1_M}z^{-1}+b_{2_M}z^{-2}+\ldots$ $A_M=1+a_{1_M}z^{-1}+\ldots$	$B_M=b_{1_M}z^{-1}+b_{2_M}z^{-2}+\ldots$ $A_M=1$	$B_M=b_{1_M}z^{-1}+b_{2_M}z^{-2}+\ldots$ $A_M=1$
$D=\frac{B_D}{A_D}$	$B_D=b_{1_D}z^{-1}+b_{2_D}z^{-2}+\ldots$ $A_D=1+a_{1_D}z^{-1}+a_{2_D}z^{-2}+\ldots$	$B_D=b_{1_D}z^{-1}+b_{2_D}z^{-2}+\ldots$ $A_D=1+a_{1_D}z^{-1}+\ldots$	$B_D=b_{1_D}z^{-1}+b_{2_D}z^{-2}+\ldots$ $A_D=1$	$B_D=b_{1_D}z^{-1}+b_{2_D}z^{-2}+\ldots$ $A_D=1+a_{1_D}z^{-1}+\ldots$
Stability condition	$\frac{A_MG}{PL}-\frac{\lambda}{2}=SPR$ $\lambda=\max\lambda_2(t)$	$\frac{A_MG}{PL}=SPR$	$G=SPR$	Unknown
Conv. condition	$\frac{A_MG}{PL}-\frac{\lambda}{2}=SPR$ $\lambda=\lambda_2$	$\frac{A_MG}{PL}=SPR$	Does not apply	$\frac{G}{P\hat{G}}=SPR$

Table 1
Comparison of algorithms for adaptive feedforward compensation in AVC with mechanical coupling

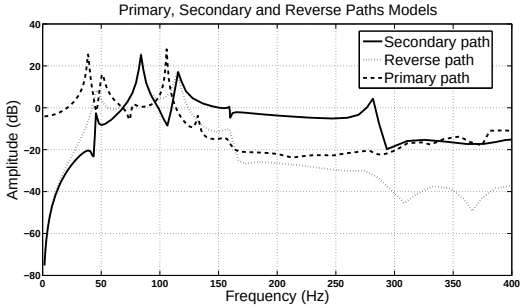

Fig. 4. Frequency characteristics of the primary, secondary and reverse paths

of $p=4$. The estimated orders of the model are $n_{B_G}=15$, $n_{A_G}=13$. The best results in terms of model validation were obtained with *Recursive Extended Least Square* method. The frequency characteristic of the secondary path is shown in figure 4 (solid). There are several very low damped vibration modes in the secondary path. The first vibration mode is at $46.56Hz$ with a damping of 0.013, the second at $83.9Hz$ with a damping of 0.011, the third one at $116Hz$ with a damping of 0.014. There is also a pair of low damped complex zeros at $108Hz$ with a damping of 0.021. There are two zeros on the unit circle corresponding to the double differentiator behavior.

The reverse path $M(q^{-1})$ has been identified in the absence of the feedforward compensator with the same PRBS excitation ($N=10$ and a frequency divider of $p=4$) applied at $\hat{y}(t)$ and measuring the output signal of the primary transducer $\hat{u}(t)$. The estimated orders of the model are $n_{B_M}=15$, $n_{A_M}=13$. The frequency characteristic of the reverse path is presented in figure 4 (dotted). There are several very low damped vibration modes at $46.20Hz$ with a damping of 0.045, at $83.9Hz$ with a damping of 0.01, at $115Hz$ with a damping of 0.014 and some additional modes in high frequencies. There are two zeros on the unit circle corresponding to the double differentiator behavior.

The primary path has been identified in the absence of the feedforward compensator using $d(t)$ as an input and measuring $\chi(t)$. The disturbance $s(t)$ was a PRBS sequence (N=10, frequency divider p=2). The estimated orders of the model are $n_{B_D}=26$, $n_{A_D}=26$. The frequency characteristic is presented in figure 4 (dashed) and may serve for simulations

and detailed performance evaluation. Note that the primary path features a strong resonance at 108 Hz, exactly where the secondary path has a pair of low damped complex zeros (almost no gain). Therefore one can not expect good attenuation around this frequency.

7.2 Broadband disturbance rejection using matrix adaptation gain

The performance of the system for rejecting broadband disturbances will be illustrated using the adaptive feedforward scheme. The adaptive filter structure for most of the experiments has been $n_R = 9$, $n_S = 10$ (total of 20 parameters) and this complexity does not allow to verify the "perfect matching condition" (not enough parameters). The influence of the number of parameters upon the performance of the system has been also investigated (up to 40 parameters).

A PRBS excitation on the global primary path will be considered as the disturbance. The corresponding spectral densities of $d(t)$ in open loop and of $\hat{u}(t)$ when feedforward compensation is active are shown in figure 5 (the effect of the mechanical feedback is significant).

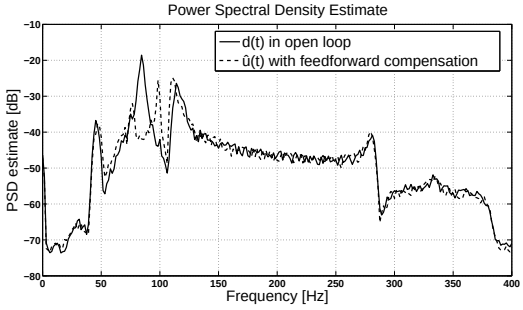

Fig. 5. Spectral densities of the image of the disturbance in open loop $d(t)$ and in feedforward compensation scheme $\hat{u}(t)$ (experimental)

For the *adaptive* operation the Algorithms *II* and *III* have been used with decreasing adaptation gain ($\lambda_1(t) = 1$, $\lambda_2(t) = 1$) combined with a *constant trace* adaptation gain [7]. Once the trace of the adaptation gain is below a given value, one switches to the constant trace gain updating. The trace of the adaptation gain $F(t)$ is maintained constant by modifying appropriately $\lambda_1(t)$ for a fixed ratio $\alpha = \lambda_1(t)/\lambda_2(t)$. The corresponding formula is:

$$trF(t+1) = \frac{1}{\lambda_1(t)} tr[F(t) - \frac{F(t)\psi(t)\psi(t)^T F(t)}{\alpha + \psi(t)^T F(t)\psi(t)}] = trF(t) \quad (62)$$

[7] Almost similar results are obtained if instead of the "decreasing adaptation gain" one uses adaptation gain updating with variable forgetting factor $\lambda_1(t)$ (the variable forgetting factor tends towards 1).

The advantage of the *constant trace* gain updating is that the adaptation moves in an optimal direction (least squares) but the size of the step does not go to zero. For details see [14,**?**].

The experiments have been carried on by first applying the disturbance and then starting the adaptive feedforward compensation after 50s. Time domain results obtained in open loop and with adaptive feedforward compensation algorithms *II* and *III* on the AVC system are shown in figure 6 and figure 7, respectively. The filter for the Algorithm *III* has been computed based on the parameter estimates obtained with algorithm *II* at t=3600s (almost same results are obtained if the initialization horizon is of the order of 200 s). The initial trace of the matrix adaptation gain for 20 parameters was 10 and the constant trace has been fixed at 0.2. As it can be seen the transient duration for Algorithm *II* is approximatively 75s seconds while for algorithm *III* is approximately 12s.

The variance of the residual force without the feedforward compensator is: $var(\chi(t) = x(t)) = 0.0354$. With adaptive feedforward compensation algorithm *II*, the variance is: $var(\chi(t)) = 0.0058$ (evaluated after 175s, when the transient is finished). This corresponds to a global attenuation of $15.68dB$ dB. Using algorithm *III* the variance of the residual acceleration is: $var(\chi(t)) = 0.0054$. This corresponds to a global attenuation of 16.23 dB, which is an improvement with respect to algorithm *II*. The convergence of the parameters is much slower (but this does not have impact on the

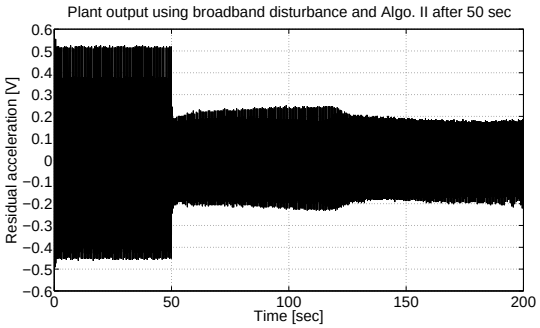

Fig. 6. Real time results obtained with Algorithm *II* using matrix adaptation gain

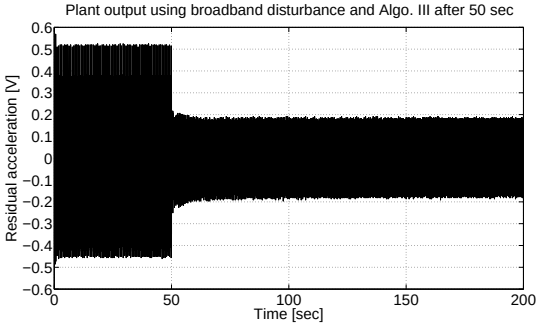

Fig. 7. Real time results obtained with Alagorithm *III* using matrix adaptation gain

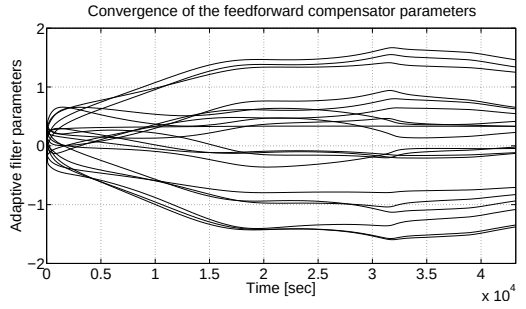

Fig. 8. Evolution of the feedforward compensator parameters for Algorithm *III* using matrix adaptation gain (experimental)

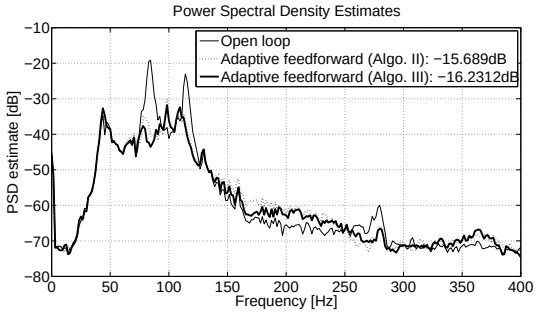

Fig. 9. Power spectral densities of the residual acceleration in open loop and with adaptive feedforward compensation (experimental)

Number of parameters	20	32	40
Global attenuation (db)	16.23	16.49	16.89

Table 2
Influence of the number of parameters upon the global attenuation

performance). This is illustrated on figure 8. The experiment has been carried over 13 hours using algorithm *III*. Figure 9 shows the power spectral densities of the residual acceleration measured on the AVC in open loop (without compensator) and using adaptive feedforward compensation (after the adaptation transient i.e. 175s). The corresponding global attenuations are also given. Algorithm *III* performs slightly better than algorithm *II*. The influence of the number of parameters upon the performance of the system is summarized in Table 2 for the case of algorithm *III*. The global attenuation is slightly improved when the number of parameters of the compensator is augmented over 20 (the PSD are almost the same).

To test the adaptive capabilities of the algorithms, a sinusoidal disturbance has been added at 1500s (adaptation algorithm III with constant trace set at 1). Figure 10 shows the time domain results in the case when the adaptation is stopped prior to the application of the sinusoidal disturbance (upper diagram) and when the adaptation is active (lower diagram). The duration of the transient is approximatively 25s. Figure 11 shows the evolution of the parameters when the sinusoidal disturbance is applied. The power spectral densities when adaptation is stopped prior to the application of the sinusoidal disturbance and when adaptation is active are shown in Figure 12. One can remark a strong attenuation of the sinusoidal disturbance (larger than $35dB$) without affecting other frequencies (similar results are obtained with algorithm *II*).

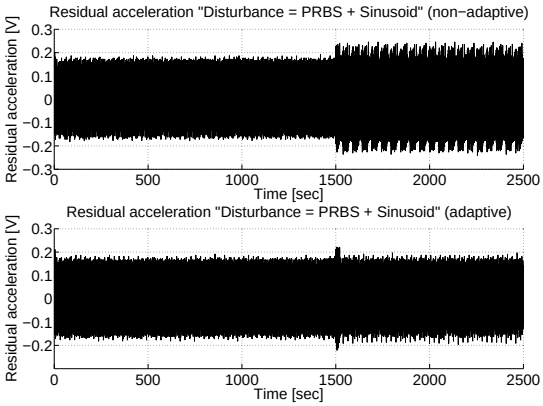

Fig. 10. Real time results for rejection of an additional sinusoidal disturbance. Upper diagram: adaptation stopped prior application of the disturbance. Lower diagram: adaptation is active

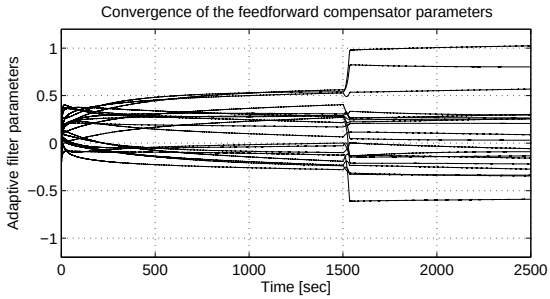

Fig. 11. Evolution of the compensator parameters when a sinusoidal disturbance is added (experimental)

7.3 Broadband disturbance rejection using scalar adaptation gain

Experiments have been carried out under the same protocol using the algorithms with scalar adaptation gain given in columns 2 (introduced in this paper), 3 ([8]) and 4 ([18]) of Table 1. The algorithm of Jacobson-Johnson (column 3) was unstable even for very low adaptation gain. The explanation

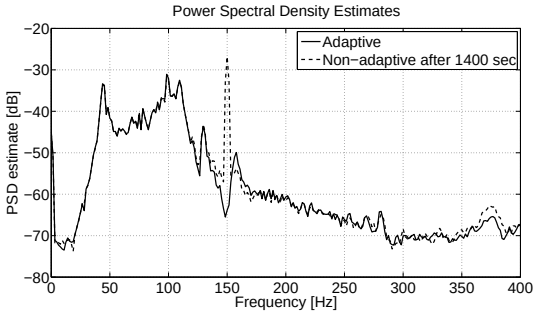

Fig. 12. Power spectral densities of the residual acceleration when an additional sinusoidal disturbance is added (Disturbance = PRBS + sinusoid)

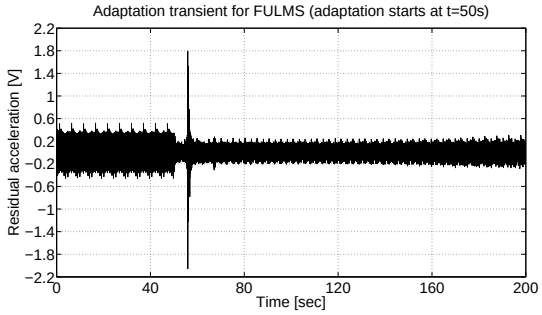

Fig. 13. Real time results obtained with FULMS algorithm

is clear. It does not use filtering at least by $\hat{G}$ and since G is not positive real (in particular in the frequency zone where most of the energy of the disturbance is concentrated) the instability is not surprising. To make a fair comparison the same adaptation gain has been used for the algorithms given in column 2 and 4 of Table 1. Since the FULMS is very sensitive to the value of the adaptation gain (becomes easily unstable and the transients are very bad) a value for the adaptation gain of 0.001 has been chosen (for a higher value FULMS is unstable). This value corresponds to a trace of a diagonal matrix adaptation gain of 0.02 when using a compensator filter with 20 parameters.

Figure 13 shows the adaptation transient for the FULMS algorithm. The maximum value is unacceptable in practice (one can not tolerate an overshoot over 30% of the uncompensated residual acceleration). Figure 14 shows the adaptation transient for the scalar version of the algorithm *III*. It is surprisingly good. Almost same transient behavior is obtained with the scalar version of algorithm *II*. Figure 15 and figure 16 show the evolution of the parameters for the FULMS algorithm and the scalar version of algorithm *III*. One can see jumps in the evolution of the parameters for the FULMS algorithms and instabilities occurs on a long run. For the algorithm *III* evolution of the parameters is smooth and no instabilities occur in a long run (12 hours). Comparing figure 16 and figure 8 one can see that the convergence point in the parameter space is not the same. Either the algorithm with scalar gain has not yet converged or there are several local minima in the case of a compensator with not enough parameters for satisfying the perfect matching condition.

The performances in the frequency domain are summarized in figure 17 where the power spectral densities and the global attenuation provided by the algorithms with scalar adaptation gain are shown. In figure 17 also the performances of a H_∞ compensator designed in [1] are also given (initial complexity: 70 parameters, reduced to 40 without loss of performance). The H_∞ design provides better performance than the FULMS but less good performance than the performance provided by algorithms *II* and *III* in their scalar or matrix version (despite that the number of filter parameters is divided by 2).
Adaptation capabilities have been tested by adding a sinusoidal disturbance like for the case of matrix adaptation gain.

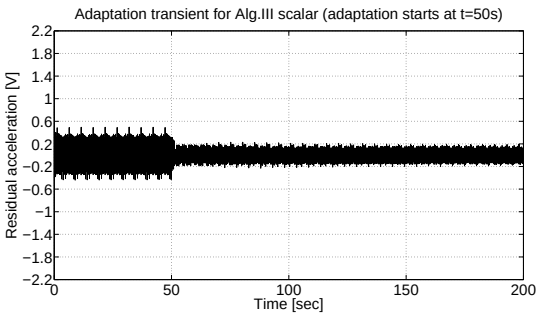

Fig. 14. Real time results obtained with Algorithm *III* using scalar adaptation gain

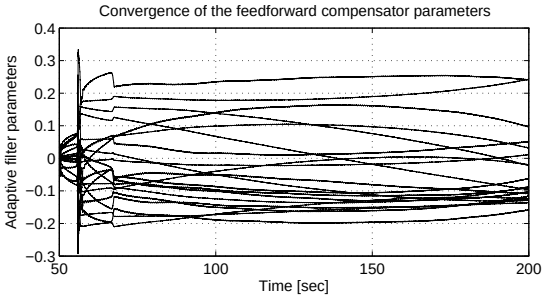

Fig. 15. Evolution of the feedforward compensator parameters (experimental) - Algorithm FULMS

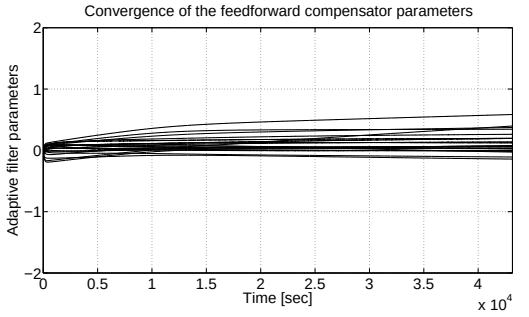

Fig. 16. Evolution of the feedforward compensator parameters (experimental) - Algorithm *III* using scalar adaptation gain

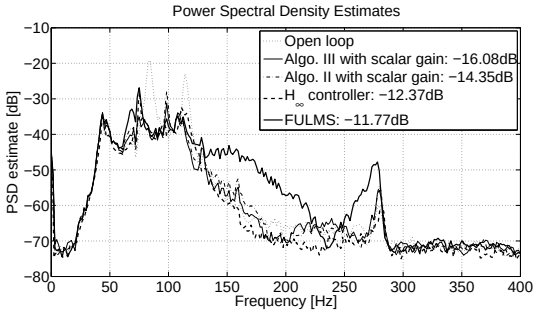

Fig. 17. Spectral densities of the residual acceleration in open loop and with adaptive feedforward compensation using scalar adaptation gain or H_∞ compensator

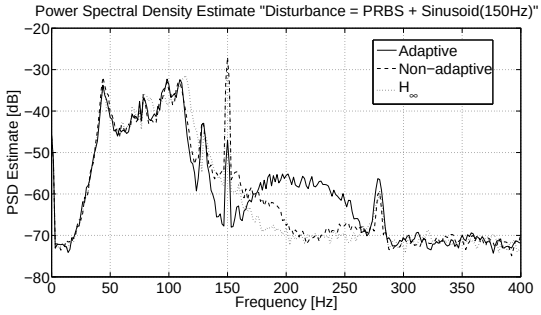

Fig. 18. Spectral densities of the residual acceleration in open loop and with adaptive feedforward compensation using scalar adaptation gain (Disturbance = PRBS + sinusoid)(experimental)

The FULMS has been destabilized by the application of the sinusoidal disturbance. Figure 18 shows the power spectral densities of the residual acceleration when the adaptation is stopped before the sinusoidal disturbance is applied, when the adaptation is active and when the H_∞ compensator (not designed for this supplementary disturbance) is used. The performance of the adaptation algorithm *III* with scalar gain is less good than in the case of matrix adaption gain (see Figure 12). The sinusoidal disturbance is attenuated in the scalar case by 20db while the attenuation is over 35dB with a matrix adaptation gain. In addition the performance is degraded in the frequency region 170-270 Hz which does not occur when using a matrix adaption gain. The H_∞ compensator does a very little attenuation of the sinuosoidal disturbance (2.6dB). It does not have "adaptation capabilities".

8 Concluding Remarks

The paper has presented several new algorithms for adaptive feedforward compensation in AVC systems taking into account the existence of an inherent internal positive feedback coupling.
Theoretical analysis has pointed out the presence of a sufficient condition for stability involving a positive real condition on a certain transfer function. This condition can be relaxed by taking into account the nature of the disturbance (broadband) or by an appropriate filtering of the regressor vector.
Real time results obtained on an active vibration control system have shown the feasibility and good performance of the proposed algorithms. The algorithms have been compared theoretically and experimentally with two other algorithms for which an analysis in the context of the internal positive feedback is available as well as with an H_∞ controller. It will be interesting to test the proposed algorithms on ANC systems.
Subjects for further research may include: 1) initialization procedures using model based designed feedforward compensators 2) imposing constraints on the poles of the internal positive feedback loop.

Appendix 1: Proof of lemma 4.1

Proof: Under the assumption H2 (perfect matching condition) the output of the primary path can be expressed as:

$$x(t) = -G(q^{-1})y(t) \tag{63}$$

where $y(t)$ is a dummy variable given by:

$$\begin{aligned} y(t+1) &= -S^*(q^{-1})y(t) + R(q^{-1})u(t+1) \\ &= \theta^T \varphi(t) = \left[\theta_S^T, \theta_R^T\right] \begin{bmatrix} \varphi_y(t) \\ \varphi_u(t) \end{bmatrix} \end{aligned} \tag{64}$$

where:

$$\theta^T = [s_1, \ldots s_{n_S}, r_0, r_1, \ldots r_{n_R}] = \left[\theta_S^T, \theta_R^T\right] \tag{65}$$

$$\begin{aligned} \varphi^T(t) &= [-y(t) \ldots -y(t-n_S+1), u(t+1) \ldots u(t-n_R+1)] \\ &= \left[\varphi_y^T(t), \varphi_u^T(t)\right] \end{aligned} \tag{66}$$

and $u(t)$ is given by:

$$u(t+1) = d(t+1) + \frac{B_M^*(q^{-1})}{A_M(q^{-1})} y(t) \tag{67}$$

For a fixed value of the parameter vector $\hat{\theta}$ characterizing the estimated filter $\hat{N}(q^{-1})$ of same dimension as the optimal filter $N(q^{-1})$, the output of the secondary path can be expressed by (in this case $\hat{z}(t) = \hat{z}^0(t)$ and $\hat{y}(t) = \hat{y}^0(t)$):

$$\hat{z}(t) = G(q^{-1})\hat{y}(t) \tag{68}$$

where:

$$\hat{y}(t+1) = \hat{\theta}^T \phi(t) \tag{69}$$

The key observation is that the dummy variable $y(t+1)$ can be expressed as:

$$\begin{aligned} y(t+1) &= \theta^T \phi(t) + \theta^T [\varphi(t) - \phi(t)] \\ &= \theta^T \phi(t) + \theta_S^T [\varphi_y - \phi_{\hat{y}}] + \theta_R^T [\varphi_u - \phi_{\hat{u}}] \end{aligned} \tag{70}$$

Define the dummy error (for a fixed vector $\hat{\theta}$)

$$\varepsilon(t+1) = y(t+1) - \hat{y}(t+1) \tag{71}$$

and the adaptation error becomes:

$$v(t+1) = -x(t) - \hat{z}(t) = G(q^{-1})\varepsilon(t+1) \tag{72}$$

It results from (70) by taking into account the expressions of $u(t)$ and $\hat{u}(t)$ given by (67) and (19) that:

$$y(t+1) = \theta^T \phi(t) - \left(S^*(q^{-1}) - \frac{R(q^{-1})B_M^*(q^{-1})}{A_M(q^{-1})} \right) \varepsilon(t) \tag{73}$$

Using equations (69) and (71), one gets (after passing all terms in ε on the left hand side):

$$\varepsilon(t+1) = \frac{A_M(q^{-1})}{P(q^{-1})}[\theta - \hat{\theta}]^T \phi(t) \tag{74}$$

Taking now into account equation(72) one obtains equation (26). End of the proof.

Appendix 2: Equivalence of notations

Present paper	In [8]	In [18]
t	k	k
D	P	G
G	C	P
B_M	F	F
A_M	1	1
N	W	C
R	$b_0 + b_1 q^{-1} + \ldots$	A
S	$1 - a_1 q^{-1} - \ldots$	B
d	s	x
$\hat{y}$	$\hat{y}$	u
$\hat{u}$	u	$x + Fu$
γ	$\frac{1}{\delta}$	γ
ϕ	ϕ	ϕ
$\psi = L\phi$	ϕ	$\hat{P}\phi$
F	$\frac{1}{\delta} I$	γI

Table 3
Present notations compared to those of [8] and [18]

References

[1] M. Alma, J.J. Martinez, I.D. Landau, and G. Buche. Design and tuning of reduced order h-infinity feedforward compensators for active vibration control. Internal report, Gipsa- Lab. INP-Grenoble.

[2] B.D.O. Anderson, R.R. Bitmead, C.R. Johnson, P.V. Kokotovic, R.L. Kosut, I.M.Y. Mareels, L. Praly, and B.D. Riedle. *Stability of adaptive systems*. The M.I.T Press, Cambridge Massachusetts , London, England, 1986.

[3] M.R. Bai and H.H.Lin. Comparison of active noise control structures in the presence of acoustical feedback by using the hinf synthesis technique. *J. of Sound and Vibration*, 206:453–471, 1997.

[4] S.J. Elliott and P.A. Nelson. Active noise control. *Noise / News International*, pages 75–98, June 1994.

[5] S.J. Elliott and T.J. Sutton. Performance of feedforward and feedback systems for active control. *IEEE Transactions on Speech and Audio Processing*, 4(3):214–223, May 1996.

[6] R. Fraanje, M. Verhaegen, and N. Doelman. Convergence analysis of the filtered-u lms algorithm for active noise control in case perfect cancellation is not possible. *Signal Processing*, 73:255–266, 1999.

[7] J Hu and J.F Linn. Feedforward active noise controller design in ducts without independent noise source measurements. *IEEE transactions on control system technology*, 8(3):443–455, 2000.

[8] C.A Jacobson, C.R Johnson, D.C Mc Cormick, and W.A Sethares. Stability of active noise control algorithms. *IEEE Signal Processing letters*, 8(3):74–76, 2001.

[9] M.S. Kuo and D.R. Morgan. *Active noise control systems-Algorithms and DSP implementation*. Wiley, New York,, 1996.

[10] M.S. Kuo and D.R. Morgan. Active noise control: A tutorial review. *Proceedings of the IEEE*, 87:943–973, 1999.

[11] I.D. Landau, A. Constantinescu, P. Loubat, D. Rey, and A. Franco. A methodology for the design of feedback active vibration control systems. *Proceedings of the European Control Conference 2001*, 2001. Porto, Portugal.

[12] I.D. Landau and A. Karimi. Recursive algorithms for identification in closed loop. a unified approach and evaluation. *Automatica*, 33(8):1499–1523, 1997.

[13] I.D. Landau, A. Karimi, and A. Constantinescu. Direct controller order reduction by identification in closed loop. *Automatica*, 37(11):1689–1702, 2001.

[14] I.D. Landau and G. Zito. *Digital Control Systems - Design, Identification and Implementation*. Springer, London, 2005.

[15] L. Ljung. On positive real transfer functions and the convergence of some recursive schemes. *IEEE Trans. on Automatic Control*, AC-22:539551, 1977.

[16] L. Ljung and T. Söderström. *Theory and practice of recursive identification*. The M.I.T Press, Cambridge Massachusetts , London, England, 1983.

[17] M. Rotunno and R.A. de Callafon. Design of model-based feedforward compensators for vibration compensation in a flexible structure. Internal report, Dept. of Mechanical and Aerospace Engineering. University of California, San Diego.

[18] A.K. Wang and W. Ren. Convergence analysis of the filtered-u algorithm for active noise control. *Signal Processing*, 73:255–266, 1999.

[19] J Zeng and R.A de Callafon. Recursive filter estimation for feedforward noise cancellation with acoustic coupling. *Journal of sound and vibration*, 291:1061–1079, 2006.